



OPEN

Implementation of a constitutive model for anisotropic rocks based on modified Lade failure criterion

Xiaotian Liu^{1,2}, Yansheng Deng^{2,3}✉ & Baoping Zou³

The strength anisotropy for inherent anisotropic rocks presents a challenge to simulate considering the influence of intermediate principal stress. Based on the modified Lade failure criterion, a new anisotropic modified Lade criterion combining an empirical equation is established and verified using published experimental datasets of anisotropic rocks. The incremental constitutive model for anisotropic rocks is derived by using finite difference theory. The dynamic link library (DLL) module of the model is obtained by using the VC++ program, and then the model is validated against various laboratory test results. It is concluded that the proposed criterion and derived model can describe the strength anisotropy of inherent anisotropic rocks well.

Abbreviations

DLL	Dynamic link library
M-C	Mohr-Coulomb
H-B	Hoek-Brown
UCS	Uniaxial compressive strength
PE	Percent error
COA	Coefficient of accordance
AAREP	Average absolute relative error percentage

Recently, some classical strength criteria for isotropic rocks in elastoplastic modeling have been continuously improved and applied by many researchers. Yao et al.¹ proposed a generalized non-linear strength theory based on the experimental data and previous achievements. In order to determine the magnitude and direction of plastic strain increment, Lu et al.² presented a three-dimensional fractional elastoplastic constitutive model for concrete material based on fractional derivative. Zhou et al.³ developed a plastic damage model with the non-orthogonal flow rule. Similarly, based on the non-orthogonal flow rule, Lu et al.⁴ proposed a cohesion-friction combined hardening plastic model, which was then implemented into ABAQUS using the implicit return mapping algorithm. Unlike isotropic rocks, anisotropic rocks such as slate, schist, gneisses, sandstone, and shale have a nonlinear strength response due to their inherent planes of anisotropy. Lots of research revealed that the loading direction β (angle between major principal direction and orientation of anisotropy plane) has a significant influence on the anisotropic strength. For most anisotropic rocks, the maximum strength has been noticed either at $\beta=0^\circ$ or 90° , while the minimum strength is usually observed at $\beta=30^\circ-45^\circ$ ⁵⁻⁷. Figure 1 presents the typical strength characteristic curves of anisotropic rock with different β . If only sliding failure is considered without non-sliding failure for anisotropic rock with a single weak plane, its strength curves often show U-shape^{5,8}. In order to consider also non-sliding failure, Jaeger and Cook⁹ improved the above-mentioned failure criterion based on M-C, which leads to a shoulder-shaped strength characteristic curve with equal strength at both sides. However, this is not consistent with most of the experimental results¹⁰. When anisotropic rock contains more than one group of weak plane, the wave shaped strength curve is always followed. If the rock with higher anisotropy, its strength characteristic curve is U-shoulder shape. Based on these studies, the failure modes of inherent anisotropic rock fall into two basic types, the sliding failure, and the non-sliding failure. The sliding failure means that failure occurs along the inherent weak plane, while the failure occurred through the rock matrix is called non-sliding failure.

¹College of Civil Engineering, Tongji University, Shanghai 200092, People's Republic of China. ²China Construction Eighth Engineering Division Corp., Ltd., Shanghai 200112, People's Republic of China. ³School of Civil Engineering and Architecture, Zhejiang University of Science and Technology, Hangzhou 310023, People's Republic of China. ✉email: ysdeng@zust.edu.cn

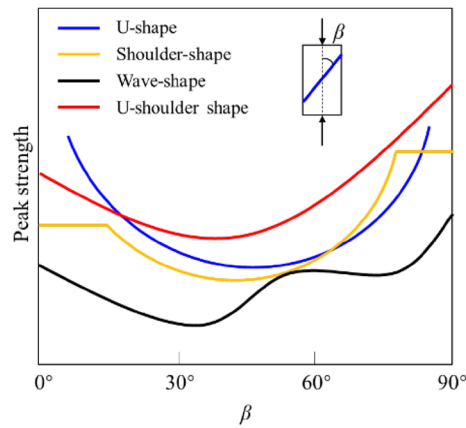


Figure 1. Strength characteristic curves of anisotropic rock with β .

Due to the special strength characteristics of anisotropic rocks, the directional variation of the strength for anisotropic rocks has been widely investigated over the last few decades^{8,11}. To describe the anisotropic strength, direct or indirect modifications are developed based on classical failure criteria such Mohr – Coulomb (M – C), Hoek – Brown (H – B) failure criterion, etc. The direct method is to introduce a new parameter into the original criterion and keep the material parameters constant in terms of their orientation^{12–14}. The indirect modification is to replace material parameters (like m or s from H – B) of the failure criterion with an empirical formula that describes the relationship between strength and the orientation angle, which was extensively studied in previous research^{15–20}. Thus, various empirical equations or approaches were proposed to describe the inherent anisotropy. Jaeger⁸ proposed the formula of cohesion of anisotropic rocks varied with the β . And later modified by Donath^{5,21}. To describe the variation of the anisotropic strength with the orientation angle, β , McLamore and Gray²² improved the Donath's equation. Hoek and Brown¹⁶ studied the relationship between the strength parameters, m_b and s , and the direction of loading. Pietruszczak and Mroz¹⁸ introduced a second-order microstructure tensor to reflect the inherent strength of anisotropy, and then Pietruszczak and Mroz¹⁹ proposed the critical plane approach to describe the direction-dependent strength for anisotropic rocks. Based on an extensive uniaxial test database, Shi et al.²⁰ proposed a modified H–B failure criterion for anisotropic rocks, and the presented empirical equation of the uniaxial compressive strength (UCS) for any β was also verified to have excellent prediction capabilities. However, the above-mentioned researches do not consider the effect of the intermediate principal stress due to the limitation of the adopted failure criteria.

In this study, a modified Lade failure criterion for anisotropic rocks was proposed and verified based on an extensive uniaxial and triaxial test database at first. Then, the three-dimensional anisotropic modified Lade model is formulated in terms of stress and strain increments. The DLL module of the model is obtained by using the VC++ program based on the finite difference theory. At last, the modified Lade model for anisotropic rocks is validated against various laboratory test results.

Problem description and basic equations

The Lade failure criterion was initially proposed by Lade for the failure of frictional materials, which describes the failure of materials using a special relationship between the first and the third invariants of the stress tensor as follows²³:

$$\left(\frac{I_1^3}{I_3} - 27\right)\left(\frac{I_1}{P_a}\right)^k = \eta \quad (1)$$

$$\begin{aligned} I_1 &= \sigma_1 + \sigma_2 + \sigma_3 \\ I_3 &= \sigma_1\sigma_2\sigma_3 \end{aligned} \quad (2)$$

where σ_1 , σ_2 , and σ_3 are the three principal stresses, I_1 and I_3 are the first and third stress tensor invariants, k and η are material constants, P_a is atmospheric pressure.

To consider the influence of the intermediate principal stress on wellbore stability in a simple methodology, the modified Lade failure criterion was proposed by Ewy²⁴, which is a simplified version of the Lade failure criterion. Similar to the M–C failure criterion, the modified Lade criterion is only governed by two most commonly used parameters: c and φ , which can be written as follows:

$$\frac{(I_1'')^3}{I_3''} = 27 + \eta \quad (3)$$

$$\begin{aligned}
 I_1'' &= (\sigma_1 + S_a - P_p) + (\sigma_2 + S_a - P_p) + (\sigma_3 + S_a - P_p) \\
 I_3'' &= (\sigma_1 + S_a - P_p)(\sigma_2 + S_a - P_p)(\sigma_3 + S_a - P_p)
 \end{aligned}
 \tag{4}$$

where I_1'' and I_3'' are the appropriate first and third stress tensor invariants. S_a and η are material constants. P_p is pore pressure. S_a represents the cohesion of rock, c , while η is determined by internal friction angle, φ . Calculations show that both S_a and η can be obtained directly from the M–C criterion c and φ by

$$S_a = \frac{c}{\tan \varphi}
 \tag{5}$$

$$\eta = 4 \tan^2 \varphi \frac{9 - 7 \sin \varphi}{1 - \sin \varphi}
 \tag{6}$$

where c and φ can be obtained by the conventional triaxial compression tests.

For anisotropic rocks such as slate, gneisses, schist, and shale, the strength highly depends on the loading direction^{7,25–27}. To predict the strength of anisotropic rocks, an indirect modification method with empirical function is widely used to modify the material strength parameters based on the orientation angle, β ^{8,15,16}. That means the strength parameters c and φ are orientation-dependent which needs assignment for each β . Thus, the anisotropic modified Lade failure criterion can be given by

$$\frac{(I_{1\beta}'')^3}{I_{3\beta}''} = 27 + \eta_\beta
 \tag{7}$$

$$\begin{aligned}
 I_{1\beta}'' &= (\sigma_1 + S_{a\beta} - P_p) + (\sigma_2 + S_{a\beta} - P_p) + (\sigma_3 + S_{a\beta} - P_p) \\
 I_{3\beta}'' &= (\sigma_1 + S_{a\beta} - P_p)(\sigma_2 + S_{a\beta} - P_p)(\sigma_3 + S_{a\beta} - P_p)
 \end{aligned}
 \tag{8}$$

$$\eta_\beta = 4 \tan^2 \varphi(\beta) \frac{9 - 7 \sin \varphi(\beta)}{1 - \sin \varphi(\beta)}
 \tag{9}$$

$$S_{a\beta} = \frac{c(\beta)}{\tan \varphi(\beta)}
 \tag{10}$$

Based on an extensive triaxial test database, the maximum UCS of anisotropic rocks is at $\beta = 90^\circ$, while the other is at $\beta = 0^\circ$. To figure out this discrepancy, Shi et al.²⁰ proposed a new empirical equation of the UCS to describe the relationship between material parameters (c and φ) and β as follows:

$$\begin{cases}
 \gamma(\beta) = \gamma_0 - (\gamma_0 - \gamma_{\min}) \left[\sin\left(\frac{90^\circ \beta}{\theta}\right) \right]^m, & 0^\circ \leq \beta \leq \theta \\
 \gamma(\beta) = \gamma_{90} - (\gamma_{90} - \gamma_{\min}) \left[\cos\left(\frac{90^\circ(\beta - \theta)}{90^\circ - \theta}\right) \right]^n, & \theta \leq \beta \leq 90^\circ
 \end{cases}
 \tag{11}$$

where γ_{\min} is the minimum value of strength parameter, γ_0 and γ_{90} are strength parameters at $\beta = 0^\circ$ and 90° , m and n are constants, and θ is the angle corresponding to the minimum strength parameter.

Among the aforementioned parameters, γ_0 , γ_{90} , γ_{\min} , m , n , and θ are the anisotropic parameters of the proposed model, which can capture the strength anisotropy. γ_0 , γ_{90} , γ_{\min} and θ can be determined directly by test results. To calibrate the remaining two parameters (m and n), the trial-and-error method can be employed to obtain the optimal solutions based on the least sum of square error (LSSE). Take the UCS of layered rock as an example provided by Zhang et al.²⁸. To cohesive, the γ_0 , γ_{90} , γ_{\min} and θ are 24.84 MPa, 28.97 MPa, 19.95 MPa and 35° , respectively, based on the test data. Substituting them into Eq. (11), m and n can be determined as 1.8 and 2.1 (LSSE is $8.0e-4$) based on trial-and-error method and LSSE. Generally, the trial-and-error method for m and n can start with a smaller integer, like 1, and then increase gradually with the interval of 0.1.

The prediction capacities of the developed anisotropic modified Lade failure criterion were analyzed and verified by three different error measures, percent error (PE) for each data point, coefficient of accordance (COA), and average absolute relative error percentage (AAREP)^{29,30}, which are given by

$$PE = \left(\frac{\sigma_{1cal} - \sigma_{1exp}}{\sigma_{1exp}} \right) \times 100\%
 \tag{12}$$

$$COA = \frac{\sum (\sigma_{1exp} - \sigma_{1cal})^2}{\sum (\sigma_{1exp} - \sigma_{1av})^2}
 \tag{13}$$

$$AAREP = \frac{\sum_{i=1}^N \left| \frac{\sigma_{1cal} - \sigma_{1exp}}{\sigma_{1exp}} \right|}{N} \times 100\% \quad (14)$$

where σ_{1cal} and σ_{1exp} are the experimental and predicted value of the major principal stress at failure for given confining pressure, σ_{1av} is the average of the experimental σ_1 for the triaxial data set under consideration, N is the total number of triaxial data points.

An extensive database³⁰ obtained from the uniaxial and triaxial tests on anisotropic rocks such as slate, shale, schist, sandstone, gneiss, phyllite, etc., were used to verify the prediction capacity. The predicted and experimental σ_1 values were presented in Fig. 2, from which all points are closely scattered about a line with a gradient of 1:1. The regression coefficient, R^2 is about 0.975, which means a good regression result. Figure 3 plots the probability distribution for PE based on Eq. (12). From Fig. 3, the probability of the PE to be within -20% to $+20\%$ is about 0.91. The probability distribution for COA is plotted in Fig. 4. The probability of COA being less than or equal to 0.1 is 0.9354 which is considerably high. In addition, the AAREP is obtained to be 11.4%, which is also relatively low. Therefore, the proposed anisotropic modified Lade failure criterion fits well not only the uniaxial tests but also the triaxial in the provided database.

Methods

The constitutive model formulation in FLAC^{3D} can be expressed as incremental form with the principal stresses $\sigma_1, \sigma_2, \sigma_3$, and the principal strains $\varepsilon_1, \varepsilon_2, \varepsilon_3$. Assuming that the compressive stress is positive, and $\bar{\sigma}_i = \sigma_i + S_a, i = 1, 2, 3$. Based on the stress tensor invariants and the partial stress tensor invariants equation (see Supplementary Appendix), the anisotropic modified Lade failure criterion can be rewritten as

$$I_1^3 - \alpha I_3 = 0 \quad (15)$$

where $\alpha = 27 + \eta$.

Substituting the relationship between stress tensor and invariants (see Supplementary Appendix) into Eq. (15) gives

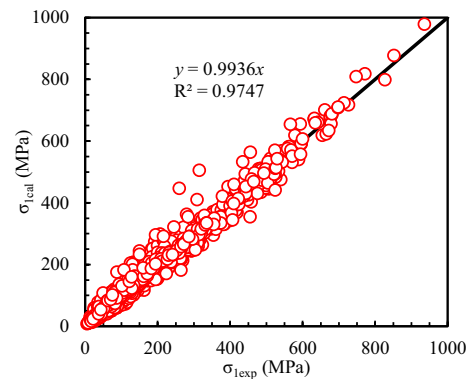


Figure 2. Predicted and Experimental σ_1 .

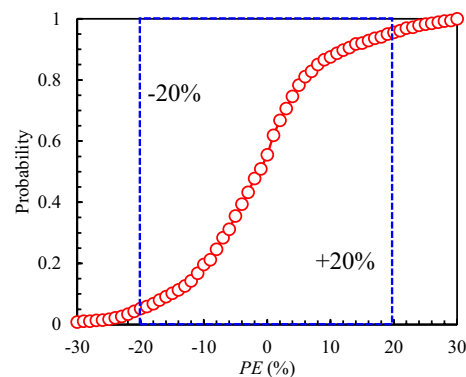


Figure 3. Probability distribution for percent error.

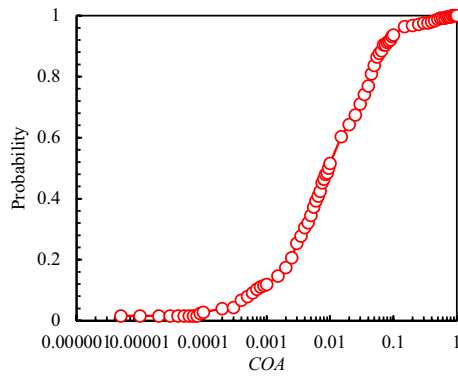


Figure 4. Probability distribution for COA.

$$\left(\frac{I_1}{\sqrt{J_2}}\right)^3 - \frac{9\alpha I_1}{(\alpha - 27)\sqrt{J_2}} - \frac{18\alpha \sin(3\theta_{\bar{\sigma}})}{\sqrt{3}(\alpha - 27)} = 0, \quad \alpha > 27 \tag{16}$$

Substituting $I_1/\sqrt{J_2} = r \sin \beta$ into Eq. (16) leads to

$$\sin^3 \beta - \frac{9\alpha}{r^2(\alpha - 27)} \sin \beta - \frac{18\alpha \sin(3\theta_{\bar{\sigma}})}{\sqrt{3}r^3(\alpha - 27)} = 0, \quad \alpha > 27 \tag{17}$$

The relationship between different angles of sine function can be obtained as follows:

$$\sin^3 \beta - \frac{3}{4} \sin \beta + \frac{1}{4} \sin(3\beta) = 0 \tag{18}$$

Comparing Eq. (16) and Eq. (17), it can be seen that

$$\begin{cases} r = 2\sqrt{\frac{3\alpha}{\alpha - 27}} \\ \sin(3\beta) = -\sqrt{\frac{\alpha - 27}{\alpha}} \sin(3\theta_{\bar{\sigma}}) \end{cases} \tag{19}$$

Therefore, Eq. (18) is a cubic equation with one variable, and its three roots are

$$\begin{cases} \left(\frac{I_1}{\sqrt{J_2}}\right)_1 = r \sin \beta = -\frac{2\sqrt{3}}{T} \sin\left(\frac{1}{3} \arcsin(T \sin(3\theta_{\bar{\sigma}}))\right) \\ \left(\frac{I_1}{\sqrt{J_2}}\right)_2 = r \sin\left(\beta - \frac{2\pi}{3}\right) = -\frac{2\sqrt{3}}{T} \sin\left(\frac{\pi}{3} - \frac{1}{3} \arcsin(T \sin(3\theta_{\bar{\sigma}}))\right) \\ \left(\frac{I_1}{\sqrt{J_2}}\right)_3 = r \sin\left(\beta + \frac{2\pi}{3}\right) = \frac{2\sqrt{3}}{T} \sin\left(\frac{\pi}{3} + \frac{1}{3} \arcsin(T \sin(3\theta_{\bar{\sigma}}))\right) \end{cases} \tag{20}$$

where $T = \sqrt{(\alpha - 27)/\alpha}$. From Eq. (20), the first root is less than or equal to 0 in the range of 0 to $\pi/6$, the second root is always less than 0 between $-\pi/6$ and $\pi/6$. Only the third root is more than or equal to 0 in the same range. Therefore, the third root is used as the solution of Eq. (20), which can be written as

$$\begin{cases} \sqrt{J_2} = \frac{TI_1}{2\sqrt{3}} g(\theta_{\bar{\sigma}}) \\ g(\theta_{\bar{\sigma}}) = \frac{1}{\sin\left(\frac{\pi}{3} + \frac{1}{3} \arcsin(T \sin(3\theta_{\bar{\sigma}}))\right)}, \quad -\frac{\pi}{6} \leq \theta_{\bar{\sigma}} \leq \frac{\pi}{6} \end{cases} \tag{21}$$

Referring to the form of generalized Mises strength criterion, Eq. (21) can be rewritten into a yield function

$$f^s = \sqrt{J_2} - 3m\bar{\sigma} \tag{22}$$

where m and σ can be expressed as

$$\begin{cases} m = \frac{Tg(\theta_{\bar{\sigma}})}{2\sqrt{3}} \\ \sigma = \frac{1}{3}I_1 \end{cases} \tag{23}$$

The total strain increment $\Delta\varepsilon_i$ consists of elastic strain increment $\Delta\varepsilon_i^e$ and plastic strain increment $\Delta\varepsilon_i^p$ (with $i = 1, 2, 3$). Based on Hooke's law, the principal stress increments can be expressed as

$$\begin{cases} \Delta\sigma_1 = S_1(\Delta\varepsilon_1^e, \Delta\varepsilon_2^e, \Delta\varepsilon_3^e) = \alpha_1\Delta\varepsilon_1^e + \alpha_2(\Delta\varepsilon_2^e + \Delta\varepsilon_3^e) \\ \Delta\sigma_2 = S_2(\Delta\varepsilon_1^e, \Delta\varepsilon_2^e, \Delta\varepsilon_3^e) = \alpha_1\Delta\varepsilon_2^e + \alpha_2(\Delta\varepsilon_1^e + \Delta\varepsilon_3^e) \\ \Delta\sigma_3 = S_3(\Delta\varepsilon_1^e, \Delta\varepsilon_2^e, \Delta\varepsilon_3^e) = \alpha_1\Delta\varepsilon_3^e + \alpha_2(\Delta\varepsilon_1^e + \Delta\varepsilon_2^e) \end{cases} \quad (24)$$

where α_1 and α_2 are material parameters, which can be given by

$$\begin{cases} \alpha_1 = K + \frac{4}{3}G \\ \alpha_2 = K - \frac{2}{3}G \end{cases} \quad (25)$$

The plastic strain increment $\Delta\varepsilon_i^p$ can be expressed by the flow rule

$$\Delta\varepsilon_i^p = \lambda \frac{\partial g^s}{\partial \sigma_i} \quad (26)$$

where λ is the plastic coefficient, g is the plastic potential function, which can be expressed by

$$g^s = \sqrt{J_2} - 3m\bar{\sigma} \quad (27)$$

Then

$$\begin{cases} \frac{\partial g^s}{\partial \sigma_1} = \frac{2\sigma_1 - \sigma_2 - \sigma_3}{6\sqrt{J_2}} - m \\ \frac{\partial g^s}{\partial \sigma_2} = \frac{2\sigma_2 - \sigma_1 - \sigma_3}{6\sqrt{J_2}} - m \\ \frac{\partial g^s}{\partial \sigma_3} = \frac{2\sigma_3 - \sigma_1 - \sigma_2}{6\sqrt{J_2}} - m \end{cases} \quad (28)$$

Combining with Eqs. (26) and (27) gives

$$\Delta\varepsilon_i^e = \Delta\varepsilon_i - \lambda \frac{\partial g^s}{\partial \sigma_i} \quad (29)$$

Substituting Eq. (29) into Eq. (24) leads to

$$\Delta\sigma_i = S_i(\Delta\varepsilon_n) - \lambda S_i \left(\frac{\partial g^s}{\partial \sigma_n} \right), \quad n = 1, 2, 3 \quad (30)$$

The new stress state σ_i^N corresponding to the total strain increment can be expressed by

$$\sigma_i^N = \sigma_i + \Delta\sigma_i \quad (31)$$

The induced elastic stresses (elastic guess) σ_i^l can be given by

$$\sigma_i^l = \sigma_i + S_i(\Delta\varepsilon_n), \quad n = 1, 2, 3 \quad (32)$$

Substituting Eqs. (28), (30) and (32) into Eq. (31) gives

$$\begin{cases} \sigma_1^N = \sigma_1^l - \left[\alpha_1 \lambda^s \left(\frac{2\sigma_1 - \sigma_2 - \sigma_3}{6\sqrt{J_2}} - m \right) + \alpha_2 \lambda^s \left(\frac{\sigma_2 + \sigma_3 - 2\sigma_1}{6\sqrt{J_2}} - 2m \right) \right] \\ \sigma_2^N = \sigma_2^l - \left[\alpha_1 \lambda^s \left(\frac{2\sigma_2 - \sigma_1 - \sigma_3}{6\sqrt{J_2}} - m \right) + \alpha_2 \lambda^s \left(\frac{\sigma_1 + \sigma_3 - 2\sigma_2}{6\sqrt{J_2}} - 2m \right) \right] \\ \sigma_3^N = \sigma_3^l - \left[\alpha_1 \lambda^s \left(\frac{2\sigma_3 - \sigma_1 - \sigma_2}{6\sqrt{J_2}} - m \right) + \alpha_2 \lambda^s \left(\frac{\sigma_1 + \sigma_2 - 2\sigma_3}{6\sqrt{J_2}} - 2m \right) \right] \end{cases} \quad (33)$$

From Eq. (33),

$$\begin{cases} \sigma^N = \sigma^l + 3mK\lambda^s \\ \sqrt{J_2}^N = \sqrt{J_2}^l - G\lambda^s \end{cases} \quad (34)$$

Substituting Eq. (34) into Eq. (22) gives

$$\lambda^s = \frac{\sqrt{J_2}^l - 3m\sigma^l}{G + 9Km^2} \quad (35)$$

The yield function of tensile stress f can be expressed by

$$f^t = \sigma - \sigma^t \tag{36}$$

Based on the associated flow rule, the potential function of tensile stress is

$$g^t = \sigma \tag{37}$$

According to Eqs. (37) and (38) can be obtained

$$\begin{cases} \frac{\partial g^t}{\partial \sigma_1} = \frac{1}{3} \\ \frac{\partial g^t}{\partial \sigma_2} = \frac{1}{3} \\ \frac{\partial g^t}{\partial \sigma_3} = \frac{1}{3} \end{cases} \tag{38}$$

Substituting Eq. (38) into Eq. (36) gives

$$\begin{cases} \sigma_1^N = \sigma_1^l - \frac{1}{3}(\alpha_1 \lambda^t + 2\alpha_2 \lambda^t) \\ \sigma_2^N = \sigma_1^l - \frac{1}{3}(\alpha_1 \lambda^t + 2\alpha_2 \lambda^t) \\ \sigma_3^N = \sigma_1^l - \frac{1}{3}(\alpha_1 \lambda^t + 2\alpha_2 \lambda^t) \end{cases} \tag{39}$$

where

$$\lambda^t = \frac{f^t}{K} = \frac{\sigma^l - \sigma^t}{K} \tag{40}$$

$H(\sigma, \sqrt{J_2}) = 0$ is designed to determine the flow rule, which can be expressed by

$$H = \sqrt{J_2} - 3m\sigma^t - (\sqrt{1 + 9m^2})(\sigma - \sigma^t) \tag{41}$$

The composite modified Lade model domains used in the definition of the flow rule are shown in Fig. 5. The failure envelope $f^s = 0$ is defined by the modified Lade model failure criterion from point A to B on Fig. 5, and by the tension failure criterion $f^t = 0$ from B to C. The diagonal line (from B to D) between the representation of $f^s = 0$ and $f^t = 0$ in the (τ, σ) plane, divides the domain of the elastic guess violating the composite yield function into two, shear failure zone and tension failure zone, respectively. If $f^s > 0$ and $H > 0$, shear failure is declared, while tension failure takes place if $f^t > 0$ and $H < 0$.

Figure 6 presents the flowchart of the proposed anisotropic modified Lade failure criterion. To apply the failure criterion to numerical simulation, a DLL module was programmed by compiling a program with C++ language, which can be read directly by FLAC^{3D}. There are two simple approaches for implementing constitutive models within FLAC^{3D} with plastic correction method³¹. In this work, an explicit form of the integration scheme of constitutive models provided by FLAC^{3D} can be utilized. A general yield criterion based on the anisotropic modified Lade failure criterion is employed, and the plastic coefficients for shear and tension can be calculated by setting the consistency condition, $g^s = 0$ and $g^t = 0$. The implementation process of the proposed model into FLAC^{3D} is as follows:

- (1) Initialize the model parameters, which is only executed once;
- (2) Obtain the total strain increment $(\Delta \epsilon_n)$, which includes the elastic and plastic components $(\Delta \epsilon_n^e$ and $\Delta \epsilon_n^p)$;

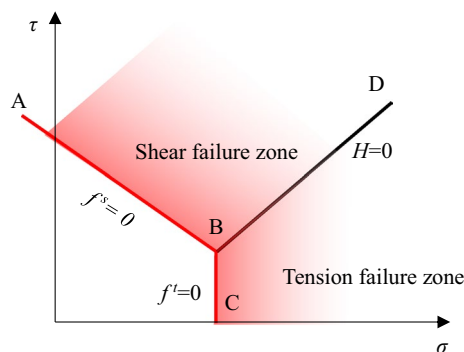


Figure 5. Modified Lade model domains used in the definition of the flow rule.

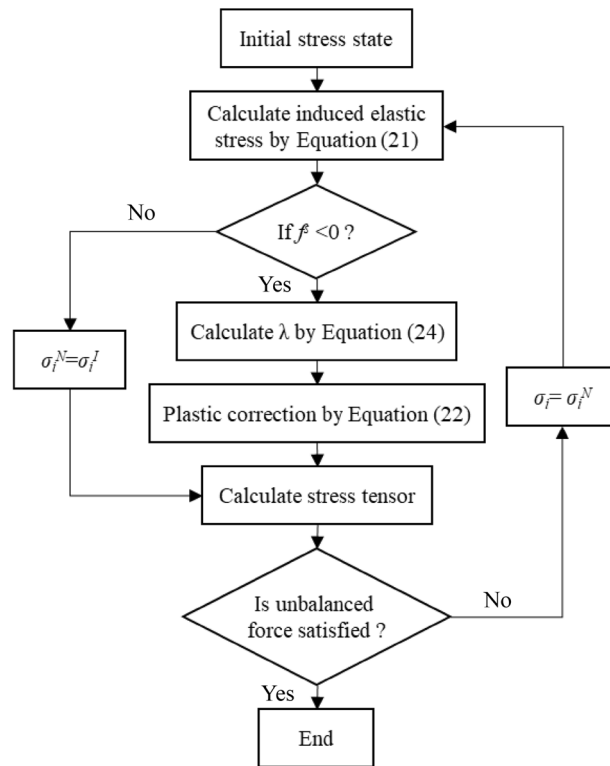


Figure 6. Flowchart of proposed model.

- (3) Calculate elastic guess σ^I at time $t + \Delta t$ using incremental elastic stress–strain law (Eq. (32)). In Eq. (32), $S_i(\Delta \epsilon_n)$ is the component i of the stress increment induced by the total-strain increment $\Delta \epsilon_n$, in case no increment of plastic deformation takes place. If the σ^I violates the yield function (Eq. (27) or Eq. (36)), Eq. (33) or Eq. (39) are used to place the new stress on the yield curve. Otherwise, σ^I gives the new stress state at time $t + \Delta t$;
- (4) If the σ^I is located above the yield surface in the generalized stress space, λ^s or λ^I are calculated in Eq. (35) or Eq. (40), and then the new stress can be obtain based on Eq. (34) or Eq. (39);
- (5) Deliver new stress to FLAC^{3D}.

Numerical results and discussion

After generating the DLL module, lots of simulations (uniaxial and triaxial compressive tests of anisotropic rocks) with the user-defined anisotropic modified Lade model were conducted to verify the correctness of the proposed model. A cylindrical rock specimen with a 100 mm height and 50 mm diameter is generated, the normal load is applied to the top, and the surface load of circumferential normal is applied to present the confining pressure. The uniaxial and triaxial test database of four different types of anisotropic rocks is used for model validation (Table 1).

A comparison between numerical and experimental results is shown in Fig. 7. The experimental results are presented as scattered points while the numerical data are plotted by solid lines. It can be seen from Fig. 7 that the shape of strength variation of different anisotropic rocks with β presents a typical U-type. Except for artificial interlayered rock, the minimum compressive strength is seen at $\beta = 30^\circ\text{--}45^\circ$, while the maximum strength is shown at $\beta = 0^\circ$ or 90° . In summary, the compressive strength predicted is consistent with the lab data of the tested anisotropic rocks under different confining stresses, indicating the rationality and correctness of the proposed model.

References	Rock type	σ_3 (MPa)	β (°)
Niandou et al. ³³	Tournemire shale	0, 5, 20, 40	0, 30, 45, 60, 90
Tien and Tsao ³⁴	Artificial interlayered rock	0, 3, 8, 15	0, 15, 30, 45, 60, 75, 90
Tien and Tsao ³⁴	Transversely isotropic rock	0, 6, 14, 35	0, 15, 30, 45, 60, 75, 90
Zhang et al. ²⁸	Layered rock	0, 10, 20, 30	0, 15, 35, 70, 90

Table 1. Uniaxial and triaxial test database for model validation.

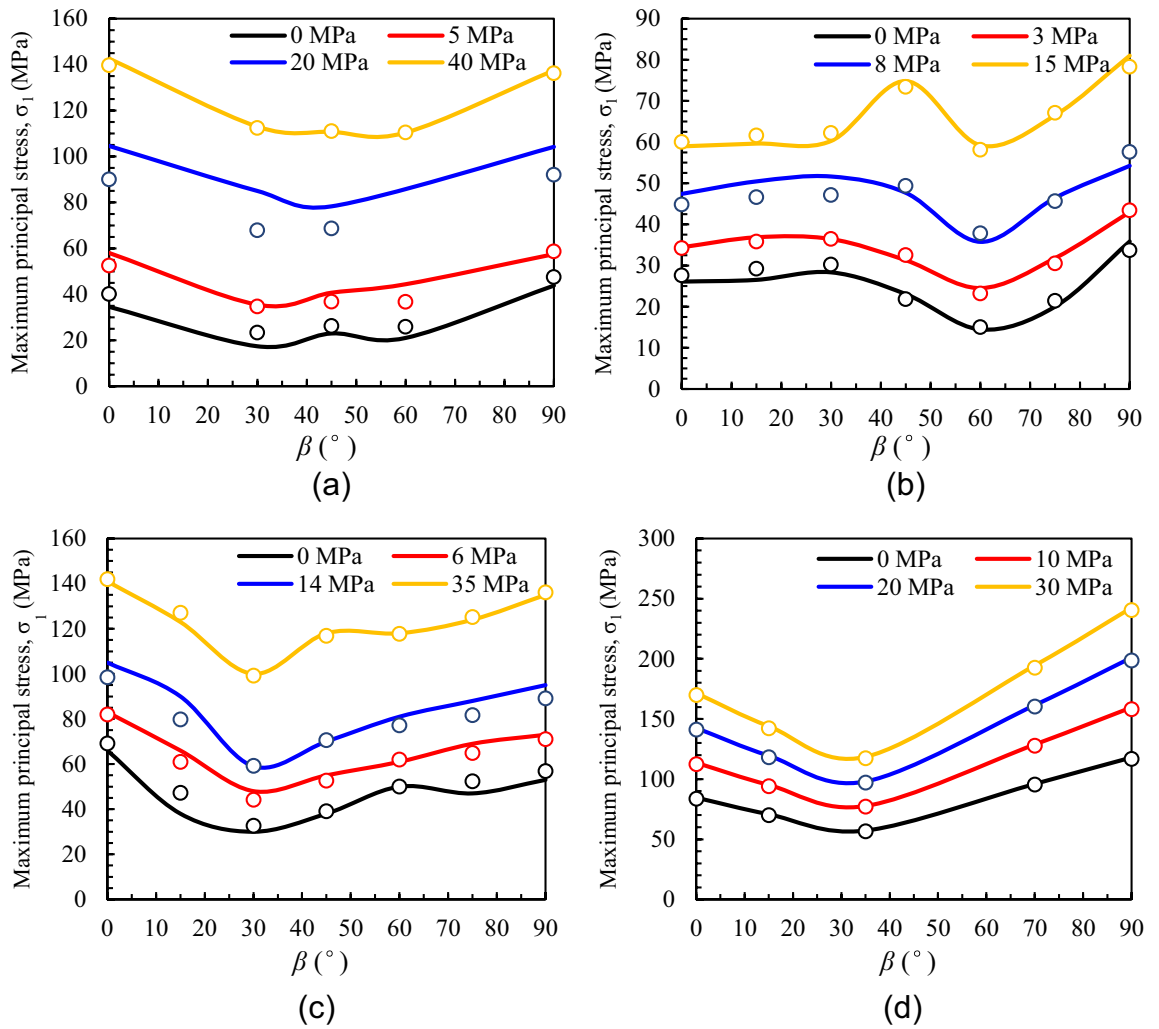


Figure 7. Comparison between numerical and experimental results: (a) Tournemire shale, (b) artificial interlayered rock, (c) transversely isotropic rock, (d) layered rock (the scattered points and solid lines represent the experimental and numerical results, respectively).

In order to reflect the advantages of proposed model in describing the rock anisotropy, a group of comparison including Donath's model, McLamore and Gray's model, and proposed model, is carried out based on the experimental data of UCS²⁸, which is shown in Fig. 8. As can be seen, the error of Donath's model is relatively large. Both the McLamore and Gray's model and proposed model can well capture the anisotropy for anisotropic

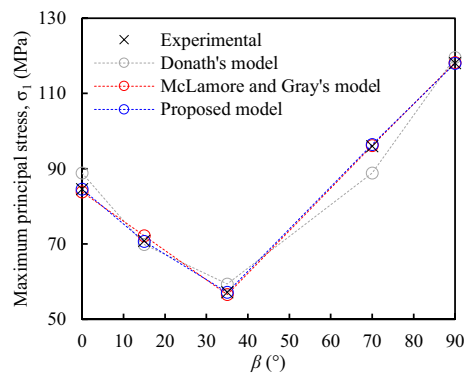


Figure 8. Comparison results between different model and experimental data.

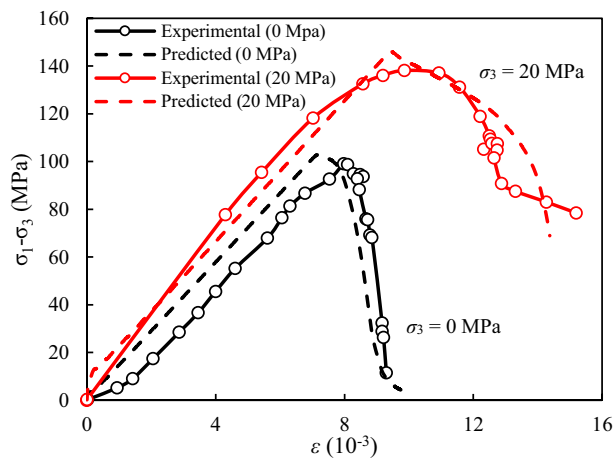


Figure 9. The complete stress–strain curves of sandstone samples ($\beta=0^\circ$) with different σ_3 from experimental and predicted results.

rock, especially at $\beta=0^\circ$, 90° , and the angle corresponding to the minimum strength. In comparison, the proposed model is more accurate in reflecting the rock anisotropy.

Additionally, to predict the complete stress–strain curves, the piecewise-linear softening law was introduced to describe the post-peak strain-softening behavior of rock³⁵. Take the triaxial compression test of sandstone specimens with $\beta=0^\circ$ presented by Zhang et al.³² as an example. The complete stress–strain curves of sandstone samples ($\beta=0^\circ$) with different σ_3 from experimental and predicted results are plotted in Fig. 9, from which the predicted stress–strain curves calculated by proposed model are basically consistent with the experimental results.

The modified Lade failure criterion describe the effect of intermediate principal stress on rock strength more correctly than M-C and Drucker-Prager criterion, and was governed by the most commonly used c and φ from the M-C failure criterion²⁴, which enhances its attractiveness for applications in engineering field. However, the modified Lade failure criterion cannot accurately describe the non-linear mechanical behavior of rock under high temperature or high pressure due to its linear nature of the shear strength envelope. Also, the proposed criterion and model in this work have similar restriction.

Conclusions

Due to the anisotropic characteristics appearing in the uniaxial or triaxial compressive test, the anisotropic modified Lade failure criterion is presented, which takes the effect of intermediate principal stress into account. The anisotropy of the rocks is considered by the variation of the parameters c_β and φ_β from the modified Lade criterion using an empirical equation. The correctness of the proposed criterion is verified by an extensive tri-axial test database.

The incremental constitutive model of the anisotropic rocks is derived based on the modified Lade failure criterion. The DLL module is developed by using the VC++ program combined with the finite difference theory. The developed model is successfully validated based on different uniaxial and triaxial compressive experiments, which shows a good agreement between numerical and experimental results under various confining pressures.

Data availability

The datasets used and/or analysed during the current study available from the corresponding author on reasonable request.

Received: 3 September 2022; Accepted: 20 February 2023

Published online: 24 February 2023

References

1. Yao, Y., Lu, D., Zhou, A. & Zou, B. Generalized non-linear strength theory and transformed stress space. *Sci. China Ser. E.* **47**, 691–709. <https://doi.org/10.1360/04ye0199> (2004).
2. Lu, D., Zhou, X., Du, X. & Wang, G. A 3D fractional elastoplastic constitutive model for concrete material. *Int. J. Solids Struct.* **165**, 160–175. <https://doi.org/10.1016/j.ijsolstr.2019.02.004> (2019).
3. Zhou, X., Lu, D., Du, X., Wang, G. & Meng, F. A 3D non-orthogonal plastic damage model for concrete. *Comput. Method. Appl. M.* **360**, 112716. <https://doi.org/10.1016/j.cma.2019.112716> (2020).
4. Lu, D., Su, C., Zhou, X., Wang, G. & Du, X. A cohesion-friction combined hardening plastic model of concrete with the non-orthogonal flow rule: Theory and numerical implementation. *Constr. Build. Mater.* **325**, 126586. <https://doi.org/10.1016/j.conbuildmat.2022.126586> (2022).
5. Donath, F.A. Strength variation and deformational behavior in anisotropic rock. in *State of Stress in the Earth's Crust.* (ed. Judd, W.R.). 281–297 (Elsevier, 1964).
6. Esamaldein, A., Wu, G., Zhao, Z. & Jiang, W. Assessments of strength anisotropy and deformation behavior of banded amphibolite rocks. *Geotech. Geol. Eng.* **32**, 429–438. <https://doi.org/10.1007/s10706-013-9724-5> (2014).

7. Tien, Y. M. & Kuo, M. C. A failure criterion for transversely isotropic rocks. *Int. J. Rock Mech. Min.* **38**, 399–412. [https://doi.org/10.1016/S1365-1609\(01\)00007-7](https://doi.org/10.1016/S1365-1609(01)00007-7) (2001).
8. Jaeger, J. C. Shear failure of anisotropic rocks. *Geol. Mag.* **97**, 65–72. <https://doi.org/10.1017/S0016756800061100> (1960).
9. Jaeger, J. C. & Cook, N. G. W. *Fundamental of Rock Mechanics* 3rd edn. (Chapman and Hall, 1979).
10. Duveau, G. & Shao, J. F. A modified single plane of weakness theory for the failure of highly stratified rocks. *Int. J. Rock Mech. Min. Sci.* **35**, 807–813 (1998).
11. Luo, Y. *et al.* Linear elastic fracture mechanics characterization of an anisotropic shale. *Sci. Rep.* **8**, 8505. <https://doi.org/10.1038/s41598-018-26846-y> (2018).
12. Bagheripour, M. H., Rahgozar, R., Pashnesaz, H. & Malekinejad, M. A complement to Hoek–Brown failure criterion for strength prediction in anisotropic rock. *Geomech. Eng.* **3**, 61–81. <https://doi.org/10.12989/gae.2011.3.1.061> (2011).
13. Ismael, M. A., Imam, H. F. & El-Shayeb, Y. A simplified approach to directly consider intact rock anisotropy in Hoek–Brown failure criterion. *J. Rock Mech. Geotech. Eng.* **6**, 486–492. <https://doi.org/10.1016/j.jrmge.2014.06.003> (2014).
14. Saroglou, H. & Tsiambaos, G. A modified Hoek–Brown failure criterion for anisotropic intact rock. *Int. J. Rock Mech. Min.* **45**, 223–234. <https://doi.org/10.1016/j.ijrmms.2007.05.004> (2008).
15. Colak, K. & Unlu, T. Effect of transverse anisotropy on the Hoek–Brown strength parameter ‘mi’ for intact rocks. *Int. J. Rock Mech. Min.* **41**, 1045–1052. <https://doi.org/10.1016/j.ijrmms.2004.04.004> (2004).
16. Hoek, E. & Brown, E. T. *Underground Excavations in Rock* (The Institute of Mining and Metallurgy, 1980).
17. Ismael, M. & Konietzky, H. Constitutive model for inherent anisotropic rocks: Ubiquitous joint model based on the Hoek–Brown failure criterion. *Comput. Geotech.* **105**, 99–109. <https://doi.org/10.1016/j.compgeo.2018.09.016> (2019).
18. Pietruszczak, S. & Mroz, Z. Formulation of anisotropic failure criteria incorporating a microstructure tensor. *Comput. Geotech.* **26**, 105–112. [https://doi.org/10.1016/S0266-352X\(99\)00034-8](https://doi.org/10.1016/S0266-352X(99)00034-8) (2000).
19. Pietruszczak, S. & Mroz, Z. On failure criteria for anisotropic cohesive–frictional materials. *Int. J. Numer. Anal. Meth. Geomech.* **25**, 509–524. <https://doi.org/10.1002/nag.141> (2001).
20. Shi, X. C., Yang, X., Meng, Y. F. & Li, G. Modified Hoek–Brown failure criterion for anisotropic rocks. *Environ. Earth Sci.* **75**, 995. <https://doi.org/10.1007/s12665-016-5810-3> (2016).
21. Donath, F. A. Experimental study of shear failure in anisotropic rock. *Geol. Soc. Am. Bull.* **72**, 985–990. [https://doi.org/10.1130/0016-7606\(1961\)72\[985:ESOSFI\]2.0.CO;2](https://doi.org/10.1130/0016-7606(1961)72[985:ESOSFI]2.0.CO;2) (1961).
22. McLamore, R. T. & Gray, K. E. A strength criterion for anisotropic rocks based upon experimental observations in *Annual Meeting of the American Institute of Mining, Metallurgical, and Petroleum Engineers, Los Angeles, California*. <https://doi.org/10.2118/1721-MS> (1967).
23. Lade, P. V. Failure criterion for frictional materials. in *Mechanics of Engineering Materials*. (eds. Desai, C.S. & Gallagher, R.H.). 385–402 (Wiley, 1984).
24. Ewy, R. T. Wellbore stability predictions by use of a modified Lade criterion. *J. Pet. Technol.* **50**, 64–66. <https://doi.org/10.2118/1198-0064-JPT> (1999).
25. Chen, C. S. & Hsu, S. C. Measurement of indirect tensile strength of anisotropic rocks by the ring test. *Rock Mech. Rock Eng.* **34**(4), 293–321. <https://doi.org/10.1007/s006030170003> (2001).
26. Nasser, M. H. B., Rao, K. S. & Ramamurthy, T. Anisotropic strength and deformational behavior of Himalayan schists. *Int. J. Rock Mech. Min.* **40**, 3–23. [https://doi.org/10.1016/S1365-1609\(02\)00103-X](https://doi.org/10.1016/S1365-1609(02)00103-X) (2003).
27. Singh, V. K., Singh, D. & Singh, T. N. Prediction of strength properties of some schistose rocks from petrographic properties using artificial neural networks. *Int. J. Rock Mech. Min.* **38**(2), 269–284. [https://doi.org/10.1016/S1365-1609\(00\)00078-2](https://doi.org/10.1016/S1365-1609(00)00078-2) (2001).
28. Zhang, Z. Z., Zhou, L. L., Yuan, Z. X. & Sun, Z. H. Research on shear failure criterion for layered rock mass. *Adv. Mater. Res.* **446–449**, 1491–1496. <https://doi.org/10.4028/www.scientific.net/AMR.446-449.1491> (2012).
29. Shen, J., Jimenez, R., Karakus, M. & Xu, C. A simplified failure criterion for intact rocks based on rock type and uniaxial compressive strength. *Rock Mech. Rock Eng.* **47**, 357–369. <https://doi.org/10.1007/s00603-013-0408-5> (2014).
30. Singh, M., Samadhiya, N. K., Kumar, A., Kumar, V. & Singh, B. A nonlinear criterion for triaxial strength of inherently anisotropic rocks. *Rock Mech. Rock Eng.* **48**, 1387–1405. <https://doi.org/10.1007/s00603-015-0708-z> (2015).
31. Shirmohammadi, A., Hajjalilue-Bonab, M. & Dadras-Ajirloo, D. Application of a simplified anisotropic constitutive model for soft structured clay on embankment failure. *Int. J. Geomech.* **21**(8), 04021125. [https://doi.org/10.1061/\(ASCE\)GM.1943-5622.0002109](https://doi.org/10.1061/(ASCE)GM.1943-5622.0002109) (2021).
32. Zhang, X.M., Yang, S.J. & Liu, B.C. Experimental study on anisotropic strength properties of sandstone. in *Proceedings of the ISRM International Symposium on Rock Mechanics, SINOROCK 2009, Hong Kong, China* (2009).
33. Niandou, H., Shao, J. F., Henry, J. P. & Fourmaintraux, D. Laboratory investigation of the mechanical behaviour of Tournemire shale. *Int. J. Rock Mech. Min.* **34**, 3–16. [https://doi.org/10.1016/S1365-1609\(97\)80029-9](https://doi.org/10.1016/S1365-1609(97)80029-9) (1997).
34. Tien, Y. M. & Tsao, P. F. Preparation and mechanical properties of artificial transversely isotropic rock. *Int. J. Rock Mech. Min.* **37**, 1001–1012. [https://doi.org/10.1016/S1365-1609\(00\)00024-1](https://doi.org/10.1016/S1365-1609(00)00024-1) (2000).
35. *Flac 3D Modeling*. (Itasca Consulting Group, 2017).

Acknowledgements

This work is supported by the Science and Technology Program of Zhejiang Province (No. 2022C35026) and the National Natural Science Foundation of China (No. 42277155 and 41907230).

Author contributions

X.L. conceived and designed the analysis, Y.D. wrote the paper, B.Z. analyzed the results. All authors reviewed the manuscript.

Competing interests

The authors declare no competing interests.

Additional information

Supplementary Information The online version contains supplementary material available at <https://doi.org/10.1038/s41598-023-30257-z>.

Correspondence and requests for materials should be addressed to Y.D.

Reprints and permissions information is available at www.nature.com/reprints.

Publisher’s note Springer Nature remains neutral with regard to jurisdictional claims in published maps and institutional affiliations.



Open Access This article is licensed under a Creative Commons Attribution 4.0 International License, which permits use, sharing, adaptation, distribution and reproduction in any medium or format, as long as you give appropriate credit to the original author(s) and the source, provide a link to the Creative Commons licence, and indicate if changes were made. The images or other third party material in this article are included in the article's Creative Commons licence, unless indicated otherwise in a credit line to the material. If material is not included in the article's Creative Commons licence and your intended use is not permitted by statutory regulation or exceeds the permitted use, you will need to obtain permission directly from the copyright holder. To view a copy of this licence, visit <http://creativecommons.org/licenses/by/4.0/>.

© The Author(s) 2023